https://doi.org/10.5194/egusphere-2026-1216
Preprint. Discussion started: 6 March 2026

Liquid Polymer Enhances Methanogenesis and Restructures Prokaryotic Communities in Freshwater Sediments

Alexander Feckler[1] (ORCID: 0000-0001-7836-4582), Eric Bollinger[1] (ORCID: 0000-0002-1279-9193), Alexandra Unik[1], Peter Mueller[1] (ORCID: 0000-0001-6974-5498), Sabine Filker[2] (ORCID: 0000-0002-4544-8277), Christian Plicht[1] (ORCID: 0009-0005-5778-1105), Zacharias Steinmetz[1] (ORCID: 0000-0001-6675-5033), Mirco Bundschuh[1] (ORCID: 0000-0003-4876-220X)

[1]RPTU University Kaiserslautern-Landau, Department of Natural and Environmental Sciences, iES Landau, Institute for Environmental Sciences, Landau, Germany
[2]RPTU University Kaiserslautern-Landau, Department of Ecology, Kaiserslautern, Germany

Correspondence to: Alexander Feckler (alexander.feckler@rptu.de)

Abstract. The widespread use of synthetic hydrophilic polymers, such as polyvinylpyrrolidone (PVP), has raised concerns about their potential effects on environmental biogeochemical processes, yet their impact on sediment ecosystems remains largely unexplored. We investigated how PVP influences methane (CH_4) production and prokaryotic community composition in freshwater sediments over a 56-day anoxic incubation. PVP exposure accelerated the onset of methanogenesis, increased maximum CH_4 production rates, and elevated maximum CH_4 concentrations. These functional changes were accompanied by shifts in bacterial communities, particularly an enrichment of fermentative Clostridia, which generate key substrates for methanogens (H_2, acetate, and formate). Nonetheless, archaeal communities, including methanogens, exhibited comparatively minor or transient responses. Mechanistically, enhanced CH_4 production likely resulted from a combination of increased substrate availability, altered redox microenvironments, and indirect reductions in competing electron acceptors. Our results suggest that PVP modifies sediment carbon cycling through complex microbial, biogeochemical, and physical interactions rather than direct toxicity to methanogens. These findings highlight the need to consider both chemical and physical effects of synthetic hydrophilic polymers on sediment microbial ecosystems and greenhouse gas emissions, and they underscore the importance of targeted studies to quantify these impacts in natural environments.

1 Introduction

The widespread use and disposal of plastic consumer products are major drivers of environmental pollution and contribute to exceeding the planetary boundary for novel entities (Arp et al., 2021; Walker and Fequet, 2023). Global plastic production has increased rapidly in recent decades, reaching approximately 400 million metric tons (Mt) annually, with over 2,489 Mt already accumulated in landfills or natural ecosystems (Brooks et al., 2018; Geyer et al., 2017). Research on plastic pollution has largely focused on solid, hydrophobic, and water-insoluble polymers, including macroplastics, microplastics, and nanoplastics (Brunning et al., 2022; Groh et al., 2023; Hartmann et al., 2019). In contrast, synthetic hydrophilic polymers (SHPs) remain

https://doi.org/10.5194/egusphere-2026-1216
Preprint. Discussion started: 6 March 2026

poorly studied, despite an annual global production volume of 36.3 Mt and their widespread use in personal care products, pharmaceuticals, industry, and agriculture (Graves et al., 2021; Wang et al., 2023). Therefore, the effects of SHPs on ecosystem structure and biogeochemical processes remain largely unknown, particularly in sediments (Steinmetz et al., 2024). Despite their widespread use and environmental occurrence, the potential for SHPs to interfere with sediment biogeochemistry remains unexplored. This is surprising given that sediments are both a likely sink for SHPs (Guezennec et al., 2015) and a central environmental compartment in which fundamental biogeochemical processes, such as carbon and greenhouse-gas cycling, occur (McClain et al., 2003; Rabaey et al., 2024). Whether SHPs can alter microbial community structure or disrupt the syntrophic pathways underlying methanogenesis is entirely unknown.

Methane (CH_4) production is one fundamental biogeochemical process in sediments with the potential for widespread effects on ecosystems due to its global warming potential and major contribution to radiative forcing (IPCC, 2021), and its substantial emissions from natural freshwaters and wetlands (Saunois et al., 2025). In sediments, CH_4 is formed as the terminal product of anaerobic organic matter degradation through a multi-step, syntrophic microbial cascade, in which the intermediate steps are performed by a diverse anaerobic microbial community and the final step is carried out by methanogenic archaea (Conrad, 2020; Megonigal et al., 2003). This syntrophic microbial cascade may experience direct exposure to anthropogenic stress, with potential consequences for community structure and CH_4 production. Similar to microplastics (He et al., 2024; Zhang et al., 2022), SHPs may affect methanogenesis by altering sediment geochemistry and microbial activity as it has been shown for water soluble organic chemicals such as antibiotics (Bollinger et al., 2021). At the same time, chemical stressors can shift microbial community composition toward more tolerant taxa (Blanck et al., 1988). Such structural changes can subsequently shape the long-term metabolic capacity of microbial communities and ultimately alter CH_4 production dynamics (Bollinger et al., 2024, 2025).

To assess the effects of SHPs on sediment-associated prokaryotic communities and their associated ecosystem functions, we exposed freshwater sediment with a natural microbial community for 56 days to four concentrations of polyvinylpyrrolidone (PVP) serving as a model SHPs. PVP represents a suitable model SHP because it is highly water soluble, chemically stable, and widely used across industrial and pharmaceutical applications (Julinová et al., 2012; Luo et al., 2021), leading to its frequent detection in aquatic environments, such as surface waters downstream of wastewater treatment plants, with measured environmental concentrations of up to 7 mg L^{-1} (Antić et al., 2011). We quantified CH_4 production under anoxic conditions through weekly measurements and thereby assessed PVP-induced functional responses over time. In parallel, we characterized the active sediment-associated prokaryotic communities using 16S rRNA metabarcoding after 7, 28 and 56 days of exposure to link functional responses to structural community changes. Based on reported effects of microplastics on CH_4 production (He et al., 2024; Zhang et al., 2022), we hypothesized that PVP exposure increases methanogenesis. We supplemented these functional measurements with structural analyses of the active sediment-associated prokaryotic community using 16S rRNA metabarcoding. aiming to link functional effects to structural changes.

https://doi.org/10.5194/egusphere-2026-1216
Preprint. Discussion started: 6 March 2026

2 Materials and methods

2.1 Sediment sampling and processing

In June 2024, we collected a fine-grained sediment from the upper 20 cm of a naturally vegetated pond at the Eusserthal Ecosystem Research Station of the RPTU University Kaiserslautern-Landau, Germany (49°25′ N, 7°96′ E), which was immediately transported to the laboratory. The pond receives water from a forest stream and supports a natural prokaryotic community (Bollinger et al., 2021). To enrich the sediment with an additional organic carbon source, we amended it with 20 g (dry weight) of *Alnus glutinosa* (L.) Gaertn. leaf powder per kg wet sediment (gravimetric water content: $\Theta_g = 2.53 \pm 0.42$ g g^{-1}). The leaves were previously collected near Landau, Germany (49°12′ N, 8°08′ E), dried at 60 °C for 24 h, and ground into a fine powder using an electric mill.

2.2 PVP treatment and quantification

We included three PVP treatments (0.5, 50, and 5,000 mg L^{-1}), prepared from PVP K30 (40 kDa, CAS 9003-39-8; Carl Roth, Karlsruhe, Germany), along with a PVP-free control. All treatments and the control were replicated 32 times. The selected concentration range reflected environmentally relevant levels reported for European surface waters receiving municipal sewage discharges (up to 0.1 mg L^{-1}) and wastewater treatment plant effluents (0.9-7 mg L^{-1}; Antić et al., 2011), whereas the higher concentrations were selected to assess concentration-dependent effects. We prepared serial dilutions of the PVP product in unfiltered pond water collected from the sediment source. Because anaerobic organic matter degradation is highly sensitive to pH (Wang et al., 1993; Zhang et al., 2010), we adjusted the test solutions to neutral pH using NaOH. We collected triplicate water samples from each treatment, including the control, on days 0, 7, and 56, and stored all samples at 4 °C until chemical analysis (Table1).

We quantified PVP by pyrolysis–gas chromatography–mass spectrometry (Py-GC/MS) followingSteinmetz et al. (Steinmetz et al., 2020). In brief, we coupled a Pyroprobe 6150 filament pyrolyzer (CDS Analytical, USA) to a Trace GC Ultra and a DSQII single quadrupole mass spectrometer (Thermo Fisher Scientific, Germany). We ultrasonicated water samples for 10 min and applied 2 µL to a quartz filter (Whatman QM-A) in a quartz tube. We dried samples at 105 °C for 3 min under helium (20 mL min^{-1}), then flash-pyrolyzed them at 550 °C for 15 s (10 K s^{-1}). We set the transfer line to 250 °C and operated the injector at 300 °C (split 1:10; helium 1.3 mL min^{-1}). We separated pyrolysates on a 30 m × 0.25 mm × 0.25 µm ZB-5MS column (Phenomenex, Germany). The oven program started at 35 °C (2 min), increased to 104 °C at 3 K min^{-1}, then to 300 °C at 50 K min^{-1}, and held for 5 min. We maintained the GC–MS transfer line at 280 °C and the ion source at 230 °C. We identified PVP pyrolysates by analyzing a 2 mg mL^{-1} aqueous standard in scan mode (m/z 45–250) using OpenChrom v1.5.0 (Wenig and Odermatt, 2010) and the NIST08 database (National Institute of Standards and Technology, n.d.). We quantified PVP via the main fragment, 1-vinyl-2-pyrrolidinone, in selective ion monitoring mode (m/z 56 and 111). We established an 11-point calibration (5–200 mg L^{-1}), measured blanks, and included quality controls (125 mg L^{-1}). The limit of quantification was 71

https://doi.org/10.5194/egusphere-2026-1216
Preprint. Discussion started: 6 March 2026

mg L^{-1}. We diluted samples 50-fold or preconcentrated them 10-fold (50 °C, redissolved in deionized water) to match the calibration range and be able to quantify PVP concentrations in the lower two treatments.

Table 1. Nominal and measured (mean ± standard deviation; n=3) PVP concentrations in the test medium on days 0, 7, and 56 of the incubation.

Nominal (mg L^{-1})	Time (d)	Measured (mg L^{-1})
0	0	< LOD
	7	< LOD
	56	< LOD
0.5	0	0.799 ± 0.007
	7	0.853 ± 0.020
	56	0.489 ± 0.050
50	0	37.7 ± 3.1
	7	8.2 ± 0.3
	56	6.9 ± 0.3
5000	0	3754 ± 67
	7	2428 ± 69
	56	2420 ± 110

2.3 Experimental setup and greenhouse gas measurements

As described by Bollinger et al. (2021) we added 5.12 ± 0.22 g (wet weight; N = 128) of carbon-spiked sediment and 30 mL of pond water containing the respective PVP concentration (i.e., 0, 0.5, 50 and 5000 mg L^{-1}; n = 32) into airtight glass microcosms. We flushed the headspace of each microcosm with nitrogen for 30 s to generate anoxic conditions, which was subsequently hermetically sealed. We incubated all vessels for 56 days in a climate-controlled cabinet (WB 345 KHFL; mytron, Germany) at 20 ± 0.2 °C in darkness (Fig. S1).

Every seven days, we quantified CH_4 by withdrawing a 100 µL headspace gas sample (V_i) from each microcosm and injected it into a cavity-enhanced absorption spectrometer (UGGA, model 915-0011, Los Gatos Research Inc., USA) operated in a closed-loop configuration. To determine the mole fraction in the headspace (x_h), we corrected the equilibrium mole fraction (x_e, ppm) of the combined sample and loop gas for the loop volume (V_l; calibrated using certified CH_4 and CO_2 reference gases; Messer Industriegase, Germany) and the background mole fraction (x_0) assuming ambient pressure in the microcosms (Eq. 1):

$$x_h = \left(\frac{V_l}{V_i}\right) \times (x_e - x_0) + x_e \quad (1)$$

https://doi.org/10.5194/egusphere-2026-1216
Preprint. Discussion started: 6 March 2026

Afterwards, we estimated the amount of dissolved CH_4 (n_w) using Henry's law (Eq. 2):

$$n_w = K_H \times x_h \times V_w \times f_1 \quad (2)$$

where V_w is the water volume, f_1 is a conversion factor (10^{-1} Pa ppm^{-1}), and K_H is Henry's law constant adjusted for the test temperature of 293.15 K (Lide, 2004; Weiss, 1974):

$$\ln\left(K_{H_{CH_4}}\right) = -115.6477 + 155.5756 \times \left(\frac{T_K}{100}\right)^{-1} + 65.2553 \times \ln\left(\frac{T_K}{100}\right)^{-1} - 6.1698 \times \left(\frac{T_K}{100}\right) \quad (3)$$

where T_K is the temperature in Kelvin.

Finally, we normalize the total amounts of CH_4 to the dry weight of sediment (m_s) in each system (Eq. 4):

$$c(CH_4) = \frac{n_w + (x_h \times V_h \times f_1) \times (R \times T)^{-1}}{m_s \times (1 + \Theta_g)^{-1}} \quad (4)$$

where V_h is the headspace volume, R is the universal gas constant, m_s and Θ_g are the wet weight and the gravimetric water content of the sediment, respectively.

2.4 RNA extraction and metabarcoding

After measuring CH_4 (and CO_2) on days 7, 28, and 56, we destructively sampled six microcosms per treatment to collect sediment for metabarcoding analyses. We immediately stored the sediment samples at -80 °C. From each sample, we extracted RNA from 2 g of sediment using the RNeasy PowerSoil Total RNA Kit (Qiagen) according to the manufacturer's protocol. We quantified RNA concentrations using a NanoDrop 2000 spectrophotometer (Thermo Fisher Scientific) and evaluated RNA integrity with a 2100 Bioanalyzer system (Agilent).

To characterize the active sediment-associated prokaryotic community, we reverse transcribed 2 µL of each RNA extract into cDNA using random primers supplied with the iScript cDNA Synthesis Kit (Bio-Rad). We then amplified the hypervariable V4 region of the 16S rRNA gene using primers 515Fm (5′-GTGYCAGCMGCCGCGGTAA-3′) and 806Rm (5′-GGACTACNVGGGTWTCTAAT-3′) (Walters et al., 2015). Each PCR used 2 µL of cDNA as template and consisted of an initial denaturation at 98 °C for 30 s, followed by 26 cycles at 98 °C for 10 s, 63 °C for 30 s, and 72 °C for 30 s, with a final extension at 72 °C for 5 min. To minimize PCR bias, each biological replicate (i.e., microcosm per treatment) was amplified in three independent PCR reactions, which were pooled to obtain one technical composite. In a second pooling step, two biological replicates were randomly combined, reducing the number of biological replicates per treatment from six to three for sequencing. Sequencing libraries were then prepared using the NEBNext Ultra DNA Library Prep Kit for Illumina (NEB,

https://doi.org/10.5194/egusphere-2026-1216
Preprint. Discussion started: 6 March 2026

USA). We assessed library quality with a 2100 Bioanalyzer system (Agilent) and the libraries were sequenced on an Illumina MiSeq platform (2 × 300 bp paired-end; StarSeq GmbH, Germany).

We processed raw reads following Bollinger et al. (2024). Briefly, we removed primers using *cutadapt* (v1.18; Martin, 2011) and analyzed reads with the *DADA2 pipeline* (Callahan et al., 2016) using the following parameters: truncLen = c(216, 183), maxEE = 1, maxN = 0 and minOverlap = 20. We detected and removed chimeras with *vsearch* (v2.13.7; Rognes et al., 2016) and assigned taxonomy to amplicon sequence variants (ASVs) using the SINTAX algorithm (Edgar, 2016) against the Greengenes reference database (v13.5; McDonald et al., 2012). We removed ASVs lacking taxonomic assignment and those with fewer than five total occurrences across all samples (Bokulich et al., 2013). The filtered ASV table, combined with taxonomy information, was used for downstream statistical analyses. We created a rarefaction curve on the final reads to confirm saturated sampling profiles across all samples (Fig. S2).

2.6 Data processing and statistics

For the statistical analysis of CH_4 production profiles, we followed the approach by Bollinger et al. (2024). Under anoxic conditions, methanogenesis typically progresses through three phases: (i) an initial, nearly linear phase in which methanogenesis is constrained by the availability of more thermodynamically favorable electron acceptors, (ii) an exponential phase driven by the activity of methanogenic Archaea, and (iii) a stagnation phase in which CH_4 production declines due to depletion of readily available substrates (Grasset et al., 2021). To characterize these growth dynamics over time (t, days), we fitted an extended form of the von Bertalanffy growth function (Eq. 5):

$$CH_4(t) = A + \frac{L-A}{(1+v e^{-k(t-\tau)})^{\frac{1}{v}}} \quad (5)$$

where A and L represent the the lower and upper asymptotes of the curve, respectively. Thus, A corresponds to the theoretical lower bound of CH_4 concentration, which is not necessarily attained at t = 0 but approximates the initial level under our experimental conditions. Parameter k describes the intrinsic rate constant governing the steepness of the increase, τ determines the temporal displacement of the curve (i.e., the location of the inflection point), and v controls the curve's symmetry. The parameter k is primarily related to the slope around the inflection point rather than directly describing how rapidly L is reached. The time required to approach L depends jointly on both k and τ. In contrast, L mainly reflects the maximum attainable concentration, which in our experiment was largely constrained by substrate availability that was equal across treatments.

The maximum CH_4 production rate (r_{max}) was afterwards calculated as (Eq. 6):

$$r_{max} = k \times (L - A) \times (1 + v)^{-\frac{v+1}{v}} \quad (6)$$

https://doi.org/10.5194/egusphere-2026-1216
Preprint. Discussion started: 6 March 2026

We built the methanogenesis models using non-linear Bayesian regression implemented in the brms package (v2.20.0; Bürkner, 2021), which interfaces with rstan (v2.32.3; Stan Development Team, 2023). We ran four Markov chains with 20,000 iterations each, a thinning interval of 10, and a warm-up of 16,000 iterations. To ensure stable sampling and model convergence, we used previously described priors (Bollinger et al., 2024). These priors were informative enough to support reliable convergence while remaining broad enough to avoid introducing bias. Sensitivity analyses revealed no bias from the priors on the posterior distributions (Fig. S3), and validity analyses showed that the models could reliably detect parameter effects (Fig. S4). We report posterior distributions for τ, r_{max}, and L using the maximum a posteriori estimate (MAP) together with the 95% highest density credible interval (CRI). We evaluated the certainty for treatment differences using Bayes factors (BF), which indicate the relative likelihood of the alternative hypothesis (H_1) versus the null hypothesis (H_0) given the observed data. For clarity and comparability across contrasts, we expressed BF values as > 1 irrespective of the direction of the effect. When all posterior samples favor H_1 over H_0 (or vice versa), BF is technically undefined but approaches infinity (Inf).

For metabarcoding analyses, we expressed taxon-specific responses as centered log-ratio (CLR) differences relative to the control, which accounts for the compositional nature of amplicon sequencing data and allows mathematically valid comparisons among taxa (Eq. 7; Aitchison, 1982; Gloor et al., 2017):

$$CLR_i = \log(RA_i + \epsilon) - \frac{1}{D}\sum_{j=1}^{D} \log\left(RA_j + \epsilon\right) \quad (7)$$

Where RA_i is the relative abundance of ASV i in a given sample (proportion of total reads), D is the total number of ASVs in the sample, RA_j is the relative abundance of ASV j in the same sample, for j = 1, 2, …, D, and $\epsilon = 10^{-6}$ was added as a pseudocount to avoid zeros. CLR differences between treatment and control reflect deviations from baseline abundances in a compositional-data-compliant manner. We removed one replicate at 5,000 mg L^{-1} on day 7 from further analyses because it was identified as an outlier using the Mahalanobis distance (Filzmoser et al., 2008). We then performed non-metric multidimensional scaling (NMDS) based on Euclidian distances of CLR-transformed ASV abundances to ordinate samples in low-dimensional space using the R package vegan (version 2.6-6.1; Oksanen et al., 2022). We evaluated differences in community structure among PVP treatments and the control using permutational multivariate analysis of variance (PERMANOVA) on the same CLR-based Euclidean distance matrix (Anderson, 2001). NMDS plots were visually scaled such that axes reflect relative differences in community composition while maintaining mathematically valid distances. To identify taxa contributing most to observed dissimilarities, we performed similarity percentage (SIMPER) analyses on CLR-transformed data, summarizing taxon-specific contributions across time points using the R package vegan (version 2.6-6.1; Oksanen et al., 2022). We conducted all data analyses in R (version 4.4.0; R Core Team, 2025).

https://doi.org/10.5194/egusphere-2026-1216
Preprint. Discussion started: 6 March 2026

3 Results

3.1 Methane production

Across all experimental treatments, including the control, the CH_4 development followed a generalized logistic growth curve (Fig. S5) progressing through the typical phases of methanogenesis under anoxic conditions (see section 2.6). Exposure to PVP, however, caused altered CH_4 production patterns compared to the PVP-free control. Specifically, at all PVP concentrations, the time until the inflection point was reached (τ) was 2 days earlier (BF = 28.6–Inf), indicating a faster transition from the initial to the exponential phase. Maximum CH_4 production rates (r_{max}) were up to 25% higher under PVP exposure compared with the control (BF = 9.5–Inf; Fig. 1). Furthermore, the maximum attainable CH_4 concentration by the end of the incubation (L) was up to 20% higher in PVP-treated samples than in the control (BF = 399–Inf; Fig. 1).

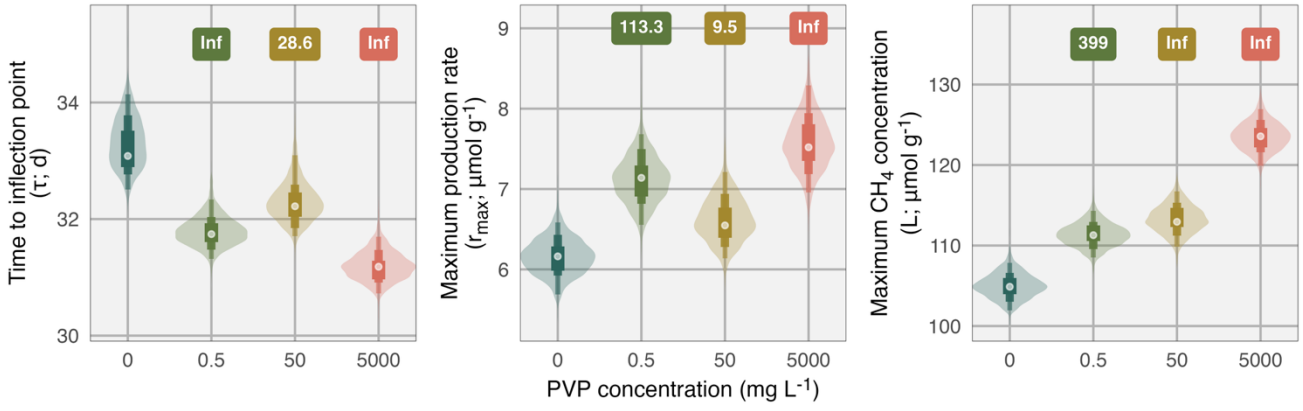

Figure 1. Violin plots showing (left) the time until the inflection point is reached (τ), (middle) the maximum CH_4 production rate (r_{max}), and (right) the maximum attainable CH_4 concentration (L) in the control and under PVP exposure. Within each violin, bars indicate the 50% (thick), 75% (medium), and 95% (slim) credible intervals, and circles mark the maximum a posteriori estimate. Bayes factors (BF) compared to the control are printed above and represent the odds ratio for the probability that the effect is greater or less than zero, with values expressed as ≥1. PVP concentrations are indicated by color: light blue = control, green = 0.5 mg L^{-1}, ochre = 50 mg L^{-1}, red = 5,000 mg L^{-1}.

3.2 Metabarcoding

A total of 9,188 ASVs from 59 phyla, 138 classes, and 206 orders were analyzed with an average of 1,233 ± 704 ASVs across 147,602 ± 42,653 reads per sample. Independent of the PVP treatment, the same prokaryotic classes (Clostridia, Bacteroidia, Proteobacteria, and Methanomicrobia) dominated all communities, despite slightly different dominance patterns among sampling times (7 days, 28 days, and 56 days; Fig. S6). Nevertheless, across all assigned prokaryotes, both PVP concentration and sampling time significantly affected the community composition (PERMANOVA; $p < 0.001$), while the PVP treatment and sampling time showed an interaction effect (PERMANOVA; $p = 0.029$; Fig. 2; Table 2). Changes in prokaryotic communities were mostly detected at the highest PVP concentration (Fig. 2). Across the three sampling times, the classes that

https://doi.org/10.5194/egusphere-2026-1216
Preprint. Discussion started: 6 March 2026

contributed most to average similarities between the highest treatment and the control were Clostridia (15.2%), Bacteroidia (12.1%), Gammaprobacteria (5.3%), Betaprobacteria (2.8%), and unassigned ASVs (2%; Fig. 2). Methanomicrobia, the prokaryotic class that contains most methanogenic archaea, also showed considerable effect sizes that revert the observed changes in CH_4 production in the exponential phase of the incubation (28 days), with negative effects at all tested PVP concentrations. However, the overall contribution of the relative abundance of these ASVs o average similarities between the highest treatment and the control was rather moderate with a dissimilarity contribution of 1.7%.

Within the phylum of Euryarcheota, effects of PVP on the community composition were less pronounced compared to the entire prokaryotic community composition (PERMANOVA; $p = 0.005$), but effect of the sampling time was consistent and significant (PERMANOVA; $p < 0.001$; Table 1). The most relevant families for dissimilarities between the highest PVP treatment and the control across samplings were Methanosarcinaceae (23.1%), Methanosaetaceae (6.2%) and Methanoregulaceae (4.4%; Fig. 2).

Table 2. PERMANOVA results for prokaryotic and Euryarchaeota community compositions. Statistical significance is highlighted in bold.

Taxa	Source of variation	Df	SumSq	F	p
Prokaryotes	Time	2	364792	4.94	**< 0.001**
	PVP	3	201469	1.82	**< 0.001**
	Time × PVP	6	271996	1.23	**0.029**
	Residual	23	849526		
	Total	34	1687783		
Euryarchaeota	Time	2	2548.5	20.9325	**< 0.001**
	PVP	3	505.7	2.77	**0.005**
	Time × PVP	6	487.9	1.34	0.133
	Residual	23	1400.1		
	Total	34	4942.3		

Df: degrees of freedom, SumSq: sums of squares

https://doi.org/10.5194/egusphere-2026-1216
Preprint. Discussion started: 6 March 2026

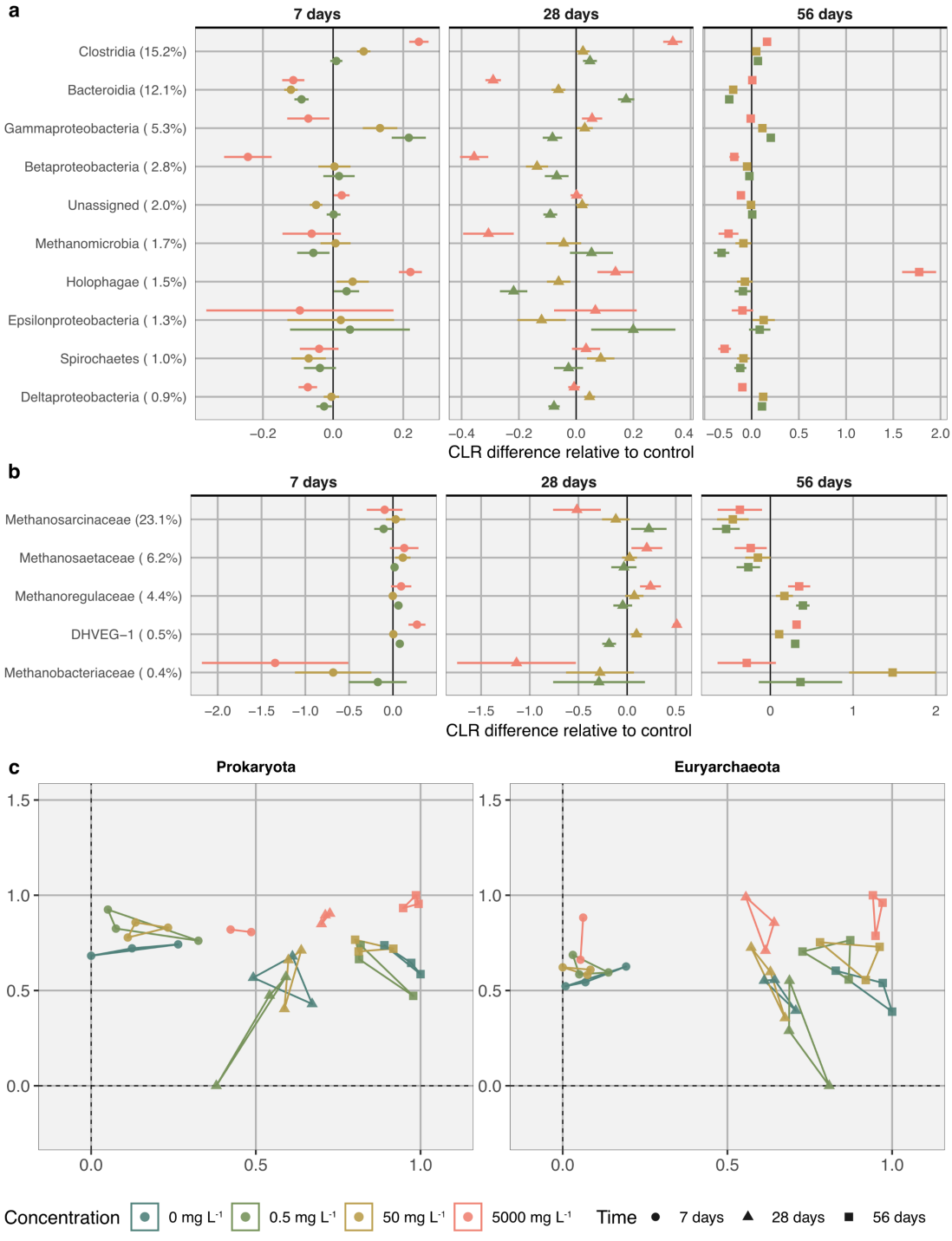

Figure 2. (a) SIMPER analysis of prokaryotes: average centered log-ratio (CLR) differences relative to the control (mean ± SE) for taxonomic classes after 7, 28, and 56 days of incubation. Negative CLR differences indicate taxa reduced relative to the control; positive values indicate taxa enriched under PVP exposure. Classes are ordered according to their contribution to the dissimilarity between the

https://doi.org/10.5194/egusphere-2026-1216
Preprint. Discussion started: 6 March 2026

highest PVP concentration (5,000 mg L^{-1}) and the control, averaged across time points, with the mean contribution (%) shown in parentheses. (b) SIMPER analysis of Euryarchaeota: average CLR differences relative to the control (mean ± SE) for taxonomic families after 7, 28, and 56 days, plotted and ordered as described for prokaryotes. (c) NMDS plots based on Euclidean distances of CLR-transformed ASV abundances. Left: prokaryotes (stress = 0.114); right: Euryarchaeota (stress = 0.008). Colors indicate PVP concentration (light blue = control, green = 0.5 mg L^{-1}, ochre = 50 mg L^{-1}, red = 5,000 mg L^{-1}), while symbols indicate sampling times (circles = 7 days, triangles = 28 days, squares = 56 days).

4 Discussion

4.1 PVP effects on methanogenesis

PVP clearly affected methanogenesis, with shorter time needed to reach the inflection point (τ), faster production rates (r_{max}), and a higher maximum attainable CH_4 concentration (L). Similar effects on τ were reported before (Bollinger et al., 2024, 2025), which have been attributed to stress-induced microbial adaptations, particularly the production of extracellular polymeric substances (EPS). Although not measured in the present study, EPS represents a well-known microbial defense response to chemical stress (Zhou et al., 2015) and can provide an additional labile carbon source for methanogens. Because its production has been reported as a response of bacteria exposed to nanoplastics (Liu et al., 2022), it may be assumed to likewise occur under PVP exposure. In addition, the increased CH_4 production under PVP exposure likely resulted from shifts in the prokaryotic community composition that altered substrate availability for methanogens. In line with this interpretation, PVP concentrations measured in the aqueous phase declined substantially over the incubation period. Although this pattern is consistent with a reduction in potential direct inhibitory effects on methanogenesis over time, the present data do not allow a clear attribution to toxicity. Alternatively, PVP may have interfered with the accessibility of electron acceptors, thereby modifying microbial competition and favouring methanogenic pathways (Rissanen et al., 2017). Such a mechanism could likewise account for both the accelerated onset and the enhanced magnitude of methane production without invoking a direct toxic mode of action.

Beyond the described microbial stress responses, PVP may reduce the effective availability of competing terminal electron acceptors. PVP has been shown to complex redox-active metals, including iron, potentially decreasing the pool of bioavailable Fe(III) in sediments (Liu et al., 2000). Such complexation could modify iron speciation, surface reactivity, or mineral–microbe interactions and thereby limit Fe(III) reduction kinetics (Shi et al., 2024). Because microbial iron reduction commonly suppresses methanogenesis when Fe(III) is abundant (Baek et al., 2019), reduced Fe(III) availability may weaken this competitive constraint and indirectly favor methanogenic pathways. However, the concomitant increase in CO_2 production under PVP exposure suggests that enhanced organic matter turnover also contributed to the observed stimulation of methanogenesis. PVP may interact with particulate organic matter or mineral surfaces, potentially disrupting aggregate structures and increasing substrate accessibility (Kleber et al., 2021; Lalonde et al., 2012; Wang et al., 2024). Increased availability of electron donors would accelerate the depletion of energetically favourable terminal electron acceptors and thereby advance the system along the redox series toward methanogenesis. In this context, the stimulation of CH_4 production

https://doi.org/10.5194/egusphere-2026-1216
Preprint. Discussion started: 6 March 2026

may arise primarily from enhanced carbon mobilization rather than from electron acceptor shielding alone. Additionally, PVP may influence the physical structure of the porewater environment. By increasing viscosity or promoting polymer-induced aggregation, PVP could restrict diffusive transport of dissolved electron acceptors within sediments (Siebel et al., 2015) and create spatial heterogeneity in redox conditions. Localized microsites may thus develop in which oxidants are rapidly depleted, creating strongly reducing conditions that favor anaerobic metabolic pathways (Lacroix et al., 2023). These microbial, biogeochemical, and physical processes are not mutually exclusive and may act interactively to sustain low-redox conditions, consistent with enhanced methanogenic activity despite the redox-inert nature of PVP. Nevertheless, the relative contribution of electron acceptor complexation, organic matter mobilization, altered porewater transport, and potential stress-induced microbial responses remains unresolved. Explicit testing of these mechanisms in targeted follow-up experiments, such as quantification of iron speciation and reduction rates, assessment of organic carbon mobilization, or determination of EPS production and sediment physical properties, is required to disentangle their respective roles.

4.2 PVP effects on prokaryotes

The overall prokaryotic community began changing early in the incubation, with effects becoming progressively more pronounced over time. In contrast, and consistent with previous observations (Bollinger et al., 2024, 2025), the ASVs within the archaeal kingdom Euryarchaeota appeared comparatively less affected. These differential responses likely reflect multiple mechanisms related to PVP binding of nutrients and metals (Liu et al., 2000), quorum-sensing molecules (i.e., bacterially released chemical signaling substances; Xue et al., 2011), and organic substances (Wang et al., 2024). First, by binding nutrients and metals, PVP alters their chemical speciation and bioavailability, selectively favoring archaea, which are generally more oligotrophic than bacteria (Sun et al., 2020). Second, sequestration of quorum-sensing molecules may disproportionately affect bacteria, which rely heavily on density-dependent signaling for growth, biofilm formation, and metabolism, whereas archaea are less dependent on quorum-sensing mechanisms (Charlesworth et al., 2017; Waters and Bassler, 2005). Third, the reduced availability of labile organic substrates may favor slow-growing oligotrophs capable of chemolithotrophy, such as archaea. Regardless of the precise mechanism, effects on bacteria likely altered interspecific interactions with archaea (Canfield et al., 2005), driving the observed community shifts, which intensified over time.

Transient adverse responses of archaeal taxa were observed during the exponential incubation phase, indicating that short-term archaeal dynamics did not directly mirror the stimulation of CH_4 production. This decoupling precludes a simple mechanistic link between archaeal community composition and methane flux. Interpretation is further constrained by the lack of functional gene expression data, which limits inference regarding the actual metabolic activity of methanogens. Moreover, given the comparatively low relative abundance of Methanomicrobia, their contribution to overall community dissimilarity was minor. Changes in archaeal composition may therefore reflect indirect responses to shifts in substrate availability (Bollinger et al., 2024) or redox conditions rather than direct effects of PVP. Broader bacterial metabolism and physicochemical alterations of the sediment environment likely represent key drivers shaping methanogenic activity. Within the bacterial domain, compositional shifts were primarily associated with members of the Clostridia. Several fermentative families

https://doi.org/10.5194/egusphere-2026-1216
Preprint. Discussion started: 6 March 2026

(Ruminococcaceae, Veillonellaceae, Lacnospiraceae, and Syntrophomonadaceae) increased under PVP exposure, particularly during the exponential phase. Clostridia are known to convert complex organic substrates into H_2, acetate, and formate, which serve as key precursors for methanogenesis (La Reau and Suen, 2018; Marchandin,bieraj and Jumas-Bilak, 2014; Sobieraj and Boone, 2006). Through syntrophic coupling, methanogens maintain low H_2 partial pressures, thereby enabling continued fermentation and efficient anaerobic carbon turnover (Mosbæk et al., 2016; Sousa et al., 2009; Westerholm et al., 2022). The proliferation of fermentative taxa is therefore consistent with enhanced substrate supply to methanogens. However, these associations should be interpreted cautiously. Relative abundance patterns do not necessarily reflect metabolic activity, and functional redundancy among taxa may obscure specific taxon-process relationships (Louca et al., 2018). Moreover, if PVP primarily altered organic matter accessibility or redox microenvironments through physicochemical effects, the observed bacterial shifts may represent secondary ecological responses rather than direct biological interactions with the polymer.

5 Conclusions

PVP exposure enhanced methanogenic activity likely through a combination of microbial, biogeochemical, and physical mechanisms. Increased substrate accessibility, altered redox microenvironments, and potential reductions in competing electron acceptors likely acted synergistically to accelerate CH_4 production, with bacterial fermenters playing a central role in supplying methanogenic substrates. Although direct toxic effects on archaea appear limited, transient community responses highlight the complex, indirect pathways by which environmental changes can shape the CH_4 flux. Importantly, such SHP-induced alterations in sediment carbon cycling could contribute to elevated natural greenhouse gas emissions, emphasizing the need to consider both chemical and physical effects of SHPs on microbial ecosystems in carbon-rich environments. Targeted follow-up experiments are required to disentangle these mechanisms and quantify their potential impact on methane and CO_2 emissions in situ.

Supplement

The supplement related to this study is available online.

Data and code availability

Data and code are publicly available on Zenodo (https://zenodo.org/records/18859767?token=eyJhbGciOiJIUzUxMiJ9.eyJpZCI6IjlhMzAzYWRmLWMxYWUtNDBhNi05YzU5LTBlOGY3MjAwMDdmMyIsImRhdGEiOnt9LCJyYW5kb20iOiIzYzA2N2NjMDY0NmRiNzYyM2Y4NTJiMjU3OTQ1NzEzYiJ9.W_2YFw64Sy18TtMpD8c8wkAuVylEBOBS1jJ5pUQDEuspMIa107-YJS9pg7kxS-

https://doi.org/10.5194/egusphere-2026-1216
Preprint. Discussion started: 6 March 2026

vJ1zMMuDtNFLfl5qdEObomfA). Raw sequencing data have been deposited at NCBI's Sequence Read Archive under accession number PRJNA1426585.

Author contributions

Conceptualization: A. Feckler, E. Bollinger, M. Bundschuh; **Data curation:** A. Feckler, **Formal analysis and visualization:** A. Feckler, E. Bollinger; **Funding acquisition:** M. Bundschuh; **Investigation:** A. Feckler, E. Bollinger, A. Unik, S. Filker, C. Plicht, Z. Steinmetz; **Methodology:** A. Feckler, E. Bollinger, S. Filker, C. Plicht, Z. Steinmetz, M. Bundschuh; **Project administration:** M. Bundschuh; **Writing – original draft:** A. Feckler; **Writing – review and editing:** E. Bollinger, A. Unik, P. Mueller, S. Filker, C. Plicht, Z. Steinmetz, M. Bundschuh

Competing interests

The authors declare there are no conflicts of interest for this manuscript.

Acknowledgements

We thank Hajar Bourassi and Simon Rudolf for laboratory assistance with sample analysis. During the preparation of this work the authors used AI (ChatGPT; GPT-5.2) to improve readability and language of the work. The authors reviewed and edited the content as needed and take full responsibility for the content of the publication.

Financial support

This study was financially supported by the research initiative "NanoKat" of the federal state of Rhineland-Palatinate, Germany.

References

Anderson, M. J.: Permutation tests for univariate or multivariate analysis of variance and regression, Can. J. Fish. Aquat. Sci., 58, 626–639, https://doi.org/10.1139/f01-004, 2001.

Antić, V. V., Antić, M. P., Kronimus, A., Oing, K., and Schwarzbauer, J.: Quantitative determination of poly(vinylpyrrolidone) by continuous-flow off-line pyrolysis-GC/MS, J. Anal. Appl. Pyrolysis., 90, 93–99, https://doi.org/10.1016/j.jaap.2010.10.011, 2011.

Arp, H. P. H., Kühnel, D., Rummel, C., MacLeod, M., Potthoff, A., Reichelt, S., Rojo-Nieto, E., Schmitt-Jansen, M., Sonnenberg, J., Toorman, E., and Jahnke, A.: Weathering plastics as a planetary boundary threat: exposure, fate, and hazards, Environ. Sci. Technol., 55, 7246–7255, https://doi.org/10.1021/acs.est.1c01512, 2021.

https://doi.org/10.5194/egusphere-2026-1216
Preprint. Discussion started: 6 March 2026

Baek, G., Kim, J., and Lee, C.: A review of the effects of iron compounds on methanogenesis in anaerobic environments, Renew. Sustain. Energy Rev., 113, 109282, https://doi.org/10.1016/j.rser.2019.109282, 2019.

Blanck, H., Wängberg, S.-Å., and Molander, S.: Pollution-induced community tolerance - a new ecotoxicological tool, Functional Testing of Aquatic Biota for Estimating Hazards of Chemicals, https://doi.org/10.1520/STP26265S, 1988.

Bokulich, N. A., Subramanian, S., Faith, J. J., Gevers, D., Gordon, J. I., Knight, R., Mills, D. A., and Caporaso, J. G.: Quality-filtering vastly improves diversity estimates from Illumina amplicon sequencing, Nat. Methods., 10, 57–59, https://doi.org/10.1038/nmeth.2276, 2013.

Bollinger, E., Zubrod, J. P., Lai, F. Y., Ahrens, L., Filker, S., Lorke, A., and Bundschuh, M.: Antibiotics as a silent driver of climate change? A case study investigating methane production in freshwater sediments, Ecotox. Environ. Saf., 228, 113025, https://doi.org/10.1016/j.ecoenv.2021.113025, 2021.

Bollinger, E., Schwilden, P., Lai, F. Y., Schulz, R., Bundschuh, M., and Filker, S.: Higher temperatures exacerbate effects of antibiotics on methanogenesis in freshwater sediment, Commun. Earth Environ., 5, 647, https://doi.org/10.1038/s43247-024-01828-3, 2024.

Bollinger, E., Mayer, J., Lai, F. Y., Schulz, R., Filker, S., and Bundschuh, M.: Adaptation of methanogenic microbial assemblages to antibiotics: The role of resistance genes and taxonomic composition, Environ. Pollut., 383, 126828, https://doi.org/10.1016/j.envpol.2025.126828, 2025.

Brooks, A. L., Wang, S., and Jambeck, J. R.: The Chinese import ban and its impact on global plastic waste trade, Sci. Adv., 4, eaat0131, https://doi.org/10.1126/sciadv.aat0131, 2018.

Brunning, H., Sallach, J. B., Zanchi, V., Price, O., and Boxall, A.: Toward a framework for environmental fate and exposure assessment of polymers, Environ. Toxicol. Chem., 41, 515–540, https://doi.org/10.1002/etc.5272, 2022.

Bürkner, P.-C.: Bayesian item response Modeling in R with brms and Stan, J. Stat. Softw., 100, 1–54, https://doi.org/10.18637/jss.v100.i05, 2021.

Callahan, B. J., McMurdie, P. J., Rosen, M. J., Han, A. W., Johnson, A. J. A., and Holmes, S. P.: DADA2: High-resolution sample inference from Illumina amplicon data, Nat. Methods, 13, 581–583, https://doi.org/10.1038/nmeth.3869, 2016.

Canfield, D. E., Erik Kristensen, and Bo Thamdrup: Structure and Growth of Microbial Populations, in: Aquatic Geomicrobiology, vol. 48, edited by: Canfield, D. E., Kristensen, E., and Thamdrup, B., Academic Press, 23–64, https://doi.org/10.1016/S0065-2881(05)48002-5, 2005.

Charlesworth, J. C., Beloe, C., Watters, C., and Burns, B. P.: Quorum Sensing in Archaea: Recent Advances and Emerging Directions, in: Biocommunication of Archaea, edited by: Witzany, G., Springer International Publishing, Cham, 119–132, https://doi.org/10.1007/978-3-319-65536-9_8, 2017.

Conrad, R.: Importance of hydrogenotrophic, aceticlastic and methylotrophic methanogenesis for methane production in terrestrial, aquatic and other anoxic environments: A mini review, Pedosphere, 30, 25–39, https://doi.org/10.1016/S1002-0160(18)60052-9, 2020.

Edgar, R. C.: SINTAX: a simple non-Bayesian taxonomy classifier for 16S and ITS sequences, bioRxiv, 074161, https://doi.org/10.1101/074161, 2016.

https://doi.org/10.5194/egusphere-2026-1216
Preprint. Discussion started: 6 March 2026

Filzmoser, P., Maronna, R., and Werner, M.: Outlier identification in high dimensions, Comput. Stat. Data Anal., 52, 1694–1711, https://doi.org/10.1016/j.csda.2007.05.018, 2008.

Geyer, R., Jambeck, J. R., and Law, K. L.: Production, use, and fate of all plastics ever made, Sci. Adv., 3, e1700782, https://doi.org/10.1126/sciadv.1700782, 2017.

Grasset, C., Moras, S., Isidorova, A., Couture, R.-M., Linkhorst, A., and Sobek, S.: An empirical model to predict methane production in inland water sediment from particular organic matter supply and reactivity, Limnol. Oceanogr., 66, 3643–3655, https://doi.org/10.1002/lno.11905, 2021.

Graves, C., Hinchclidde, T., Johnson, N., Noakes, D., and Williams, S.: Polymers in liquid formulations: a landscape view of the global PLFs market, Royal Society of Chemistry, 2021.

Groh, K. J., Arp, H. P. H., MacLeod, M., and Wang, Z.: Assessing and managing environmental hazards of polymers: historical development, science advances and policy options, Environ. Sci.: Processes Impacts, 25, 10–25, https://doi.org/10.1039/D2EM00386D, 2023.

Guezennec, A. G., Michel, C., Bru, K., Touze, S., Desroche, N., Mnif, I., and Motelica-Heino, M.: Transfer and degradation of polyacrylamide-based flocculants in hydrosystems: a review, Environ. Sci. Pollut. Res., 22, 6390–6406, https://doi.org/10.1007/s11356-014-3556-6, 2015.

Hartmann, N. B., Hüffer, T., Thompson, R. C., Hassellöv, M., Verschoor, A., Daugaard, A. E., Rist, S., Karlsson, T., Brennholt, N., Cole, M., Herrling, M. P., Hess, M. C., Ivleva, N. P., Lusher, A. L., and Wagner, M.: Are we speaking the same language? Recommendations for a definition and categorization framework for plastic debris, Environ. Sci. Technol., 53, 1039–1047, https://doi.org/10.1021/acs.est.8b05297, 2019.

He, Y., Li, Y., Yang, X., Liu, Y., Guo, H., Wang, Y., Zhu, T., Tong, Y., Ni, B.-J., and Liu, Y.: Biodegradable microplastics aggravate greenhouse gas emissions from urban lake sediments more severely than conventional microplastics, Water Res., 266, 122334, https://doi.org/10.1016/j.watres.2024.122334, 2024.

IPCC: Climate Change 2021 – the Physical Science Basis: Working Group I Contribution to the Sixth Assessment Report of the Intergovernmental Panel on Climate Change, first edition, Cambridge University Press, 2021.

Julinová, M., Kupec, J., Houser, J., Slavík, R., Marušincová, H., Červeňáková, L., and Klívar, S.: Removal of polyvinylpyrrolidone from wastewater using different methods, Water Environ. Res., 84, 2123–2132, https://doi.org/10.2175/106143012X13373575830999, 2012.

Kleber, M., Bourg, I. C., Coward, E. K., Hansel, C. M., Myneni, S. C. B., and Nunan, N.: Dynamic interactions at the mineral–organic matter interface, Nat. Rev. Earth Environ., 2, 402–421, https://doi.org/10.1038/s43017-021-00162-y, 2021.

La Reau, A. J. and Suen, G.: The Ruminococci: key symbionts of the gut ecosystem, J Microbiol., 56, 199–208, https://doi.org/10.1007/s12275-018-8024-4, 2018.

Lacroix, E. M., Aeppli, M., Boye, K., Brodie, E., Fendorf, S., Keiluweit, M., Naughton, H. R., Noël, V., and Sihi, D.: Consider the anoxic microsite: acknowledging and appreciating spatiotemporal redox heterogeneity in soils and sediments, ACS Earth Space Chem., 7, 1592–1609, https://doi.org/10.1021/acsearthspacechem.3c00032, 2023.

Lalonde, K., Mucci, A., Ouellet, A., and Gélinas, Y.: Preservation of organic matter in sediments promoted by iron, Nature, 483, 198–200, https://doi.org/10.1038/nature10855, 2012.

https://doi.org/10.5194/egusphere-2026-1216
Preprint. Discussion started: 6 March 2026

Lide, D. R.: CRC Handbook of Chemistry and Physics, CRC Press, 2004.

Liu, M., Yan, X., Liu, H., and Yu, W.: An investigation of the interaction between polyvinylpyrrolidone and metal cations, React. Funct. Polym., 44, 55–64, https://doi.org/10.1016/S1381-5148(99)00077-2, 2000.

Liu, X., Li, Y., Tang, J., Wang, D., Guo, S., Liu, Q., and Giesy, J. P.: Nano- and microplastics aided by extracellular polymeric substances facilitate the conjugative transfer of antibiotic resistance genes in bacteria, ACS EST Water, 2, 2528–2537, https://doi.org/10.1021/acsestwater.2c00330, 2022.

Louca, S., Polz, M. F., Mazel, F., Albright, M. B. N., Huber, J. A., O'Connor, M. I., Ackermann, M., Hahn, A. S., Srivastava, D. S., Crowe, S. A., Doebeli, M., and Parfrey, L. W.: Function and functional redundancy in microbial systems, Nat. Ecol. Evol., 2, 936–943, https://doi.org/10.1038/s41559-018-0519-1, 2018.

Luo, Y., Hong, Y., Shen, L., Wu, F., and Lin, X.: Multifunctional role of polyvinylpyrrolidone in pharmaceutical formulations, AAPS PharmSciTech, 22, 34, https://doi.org/10.1208/s12249-020-01909-4, 2021.

Marchandin,bieraj, H. and Jumas-Bilak, E. R.: The family Veillonellaceae, in: The Prokaryotes, edited by: Dworkin, M., Falkow, S., Rosenberg, E., Schleifer, K.-H., and Stackebrandt, E., Springer, Berlin, Heidelberg, 433–453, 2014.

Martin, M.: Cutadapt removes adapter sequences from high-throughput sequencing reads, EMB.net Journal, 17, 10–12, 2011.

McClain, M. E., Boyer, E. W., Dent, C. L., Gergel, S. E., Grimm, N. B., Groffman, P. M., Hart, S. C., Harvey, J. W., Johnston, C. A., Mayorga, E., McDowell, W. H., and Pinay, G.: Biogeochemical hot spots and hot moments at the interface of terrestrial and aquatic ecosystems, Ecosyst., 6, 301–312, 2003.

McDonald, D., Price, M. N., Goodrich, J., Nawrocki, E. P., DeSantis, T. Z., Probst, A., Andersen, G. L., Knight, R., and Hugenholtz, P.: An improved Greengenes taxonomy with explicit ranks for ecological and evolutionary analyses of bacteria and archaea, ISME J., 6, 610–618, https://doi.org/10.1038/ismej.2011.139, 2012.

Megonigal, J. P., Hines, M. E., and Visscher, P. T.: 8.08 - Anaerobic Metabolism: Linkages to Trace Gases and Aerobic Processes, in: Treatise on Geochemistry, edited by: Holland, H. D. and Turekian, K. K., Pergamon, Oxford, 317–424, https://doi.org/10.1016/B0-08-043751-6/08132-9, 2003.

Mosbæk, F., Kjeldal, H., Mulat, D. G., Albertsen, M., Ward, A. J., Feilberg, A., and Nielsen, J. L.: Identification of syntrophic acetate-oxidizing bacteria in anaerobic digesters by combined protein-based stable isotope probing and metagenomics, ISME J., 10, 2405–2418, https://doi.org/10.1038/ismej.2016.39, 2016.

National Institute of Standards and Technology: NIST Inorganic Crystal Structure Database, NIST Standard Reference Database Number 3, https://doi.org/10.18434/M32147

Oksanen, J., Simpson, G. L., Blanchet, F. G., Kindt, R., Legendre, P., Minchin, P. R., O'Hara, R. B., Solymos, P., Stevens, M. H. H., Szoecs, E., Wagner, H., Barbour, M., Bedward, M., Bolker, B., Borcard, D., Carvalho, G., Chirico, M., De Caeres, M., Durand, S., Antoniazi Evangelista, H. B., FitzJohn, R., Friendly, M., Furneaux, B., Hannigan, G., Hill, M. O., Lahti, L., McGlinn, D., Ouellette, M.-H., Ribeiro Cunha, E., Smith, T., Stier, A., Ter Braak, C. J. F., and Weedon, J.: vegan: community ecology package, 2022.

Persson, L., Carney Almroth, B. M., Collins, C. D., Cornell, S., de Wit, C. A., Diamond, M. L., Fantke, P., Hassellöv, M., MacLeod, M., Ryberg, M. W., Søgaard Jørgensen, P., Villarrubia-Gómez, P., Wang, Z., and Hauschild, M. Z.: Outside the safe operating space of the planetary boundary for novel entities, Environ. Sci. Technol., 56, 1510–1521, https://doi.org/10.1021/acs.est.1c04158, 2022.

https://doi.org/10.5194/egusphere-2026-1216
Preprint. Discussion started: 6 March 2026

R Core Team: R: a language and environment for statistical computing, 2025.

Rabaey, J. S., Holgerson, M. A., Richardson, D. C., Andersen, M. R., Bansal, S., Bortolotti, L. E., Cotner, J. B., Hornbach, D. J., Martinsen, K. T., Moody, E. K., and Schloegel, O. F.: Freshwater biogeochemical hotspots: high primary production and ecosystem respiration in shallow waterbodies, Geophys. Res. Lett., 51, e2023GL106689, https://doi.org/10.1029/2023GL106689, 2024.

Rissanen, A. J., Karvinen, A., Nykänen, H., Peura, S., Tiirola, M., Mäki, A., and Kankaala, P.: Effects of alternative electron acceptors on the activity and community structure of methane-producing and consuming microbes in the sediments of two shallow boreal lakes, FEMS Microbiol. Ecol., 93, fix078, https://doi.org/10.1093/femsec/fix078, 2017.

Rognes, T., Flouri, T., Nichols, B., Quince, C., and Mahé, F.: VSEARCH: a versatile open source tool for metagenomics, PeerJ, https://doi.org/10.7717/peerj.2584, 2016.

Saunois, M., Martinez, A., Poulter, B., Zhang, Z., Raymond, P. A., Regnier, P., Canadell, J. G., Jackson, R. B., Patra, P. K., Bousquet, P., Ciais, P., Dlugokencky, E. J., Lan, X., Allen, G. H., Bastviken, D., Beerling, D. J., Belikov, D. A., Blake, D. R., Castaldi, S., Crippa, M., Deemer, B. R., Dennison, F., Etiope, G., Gedney, N., Höglund-Isaksson, L., Holgerson, M. A., Hopcroft, P. O., Hugelius, G., Ito, A., Jain, A. K., Janardanan, R., Johnson, M. S., Kleinen, T., Krummel, P. B., Lauerwald, R., Li, T., Liu, X., McDonald, K. C., Melton, J. R., Mühle, J., Müller, J., Murguia-Flores, F., Niwa, Y., Noce, S., Pan, S., Parker, R. J., Peng, C., Ramonet, M., Riley, W. J., Rocher-Ros, G., Rosentreter, J. A., Sasakawa, M., Segers, A., Smith, S. J., Stanley, E. H., Thanwerdas, J., Tian, H., Tsuruta, A., Tubiello, F. N., Weber, T. S., van der Werf, G. R., Worthy, D. E. J., Xi, Y., Yoshida, Y., Zhang, W., Zheng, B., Zhu, Q., Zhu, Q., and Zhuang, Q.: Global Methane Budget 2000–2020, Earth Syst. Sci. Data, 17, 1873–1958, https://doi.org/10.5194/essd-17-1873-2025, 2025.

Shi, T., Peng, C., Lu, L., Yang, Z., Wu, Y., Wang, Z., and Kappler, A.: Response of Fe(III)-reducing kinetics, microbial community structure and Fe(III)-related functional genes to Fe(III)-organic matter complexes and ferrihydrite in lake sediment, Biogeochemistry, 167, 1553–1565, https://doi.org/10.1007/s10533-024-01186-4, 2024.

Siebel, D., Scharfer, P., and Schabel, W.: Determination of concentration-dependent diffusion coefficients in polymer–solvent systems: analysis of concentration profiles measured by raman spectroscopy during single drying experiments excluding boundary conditions and phase equilibrium, Macromolecules, 48, 8608–8614, https://doi.org/10.1021/acs.macromol.5b02144, 2015.

Sobieraj, M. and Boone, D. R.: Syntrophomonadaceae, in: The Prokaryotes: Volume 4: Bacteria: Firmicutes, Cyanobacteria, edited by: Dworkin, M., Falkow, S., Rosenberg, E., Schleifer, K.-H., and Stackebrandt, E., Springer US, New York, NY, 1041–1049, https://doi.org/10.1007/0-387-30744-3_37, 2006.

Sousa, D. Z., Smidt, H., Alves, M. M., and Stams, A. J. M.: Ecophysiology of syntrophic communities that degrade saturated and unsaturated long-chain fatty acids, FEMS Microbiol. Ecol., 68, 257–272, https://doi.org/10.1111/j.1574-6941.2009.00680.x, 2009.

Stan Development Team: RStan: the R interface to Stan. R package version 2.32.3, 2023.

Steinmetz, Z., Kintzi, A., Muñoz, K., and Schaumann, G. E.: A simple method for the selective quantification of polyethylene, polypropylene, and polystyrene plastic debris in soil by pyrolysis-gas chromatography/mass spectrometry, J. Anal. Appl. Pyrolysis, 147, 104803, https://doi.org/10.1016/j.jaap.2020.104803, 2020.

Steinmetz, Z., Plicht, C., Buchmann, C., Knott, M., Meyer, M., Müller-Schüssele, S., Strieth, D., Prosenc, M. H., Steinmetz, H., Jungkunst, H. F., Thiel, W. R., and Bundschuh, M.: Plastic problem solved? Environmental implications of synthetic

https://doi.org/10.5194/egusphere-2026-1216
Preprint. Discussion started: 6 March 2026

hydrophilic polymers across ecosystem boundaries, Trends Anal. Chem., 181, 118000, https://doi.org/10.1016/j.trac.2024.118000, 2024.

Sun, Y., Liu, Y., Pan, J., Wang, F., and Li, M.: Perspectives on cultivation strategies of archaea, Microb. Ecol., 79, 770–784, https://doi.org/10.1007/s00248-019-01422-7, 2020.

Walker, T. R. and Fequet, L.: Current trends of unsustainable plastic production and micro(nano)plastic pollution, Trends Anal. Chem., 160, 116984, https://doi.org/10.1016/j.trac.2023.116984, 2023.

Walters, W., Hyde Embriette R., Berg-Lyons Donna, Ackermann Gail, Humphrey Greg, Parada Alma, Gilbert Jack A., Jansson Janet K., Caporaso J. Gregory, Fuhrman Jed A., Apprill Amy, and Knight Rob: Improved bacterial 16S rRNA gene (V4 and V4-5) and fungal internal transcribed spacer marker gene primers for microbial community surveys, mSystems, 1, 10.1128/msystems.00009-15, https://doi.org/10.1128/msystems.00009-15, 2015.

Wang, X., Xu, Y., Ou, Q., Chen, W., van der Meer, W., and Liu, G.: Adsorption characteristics and mechanisms of water-soluble polymers (PVP and PEG) on kaolin and montmorillonite minerals, J. Haz. Mat., 466, 133592, https://doi.org/10.1016/j.jhazmat.2024.133592, 2024.

Wang, Z. P., DeLaune, R. D., Patrick Jr., W. H., and Masscheleyn, P. H.: Soil redox and pH effects on methane production in a flooded rice soil, Soil Sci. Soc. Am. J., 57, 382–385, https://doi.org/10.2136/sssaj1993.03615995005700020016x, 1993.

Waters, C. M. and Bassler, B. L.: QUORUM SENSING: Cell-to-cell dommunication in bacteria, Ann. Rev. Cell Dev. Biol., 21, 319–346, https://doi.org/10.1146/annurev.cellbio.21.012704.131001, 2005.

Weiss, R. F.: Carbon dioxide in water and seawater: the solubility of a non-ideal gas, Mar. Chem., 2, 203–215, https://doi.org/10.1016/0304-4203(74)90015-2, 1974.

Wenig, P. and Odermatt, J.: OpenChrom: a cross-platform open source software for the mass spectrometric analysis of chromatographic data, BMC Bioinform., 11, 405, https://doi.org/10.1186/1471-2105-11-405, 2010.

Westerholm, M., Calusinska, M., and Dolfing, J.: Syntrophic propionate-oxidizing bacteria in methanogenic systems, FEMS Microbiol. Rev., 46, fuab057, https://doi.org/10.1093/femsre/fuab057, 2022.

Xue, X., Pasparakis, G., Halliday, N., Winzer, K., Howdle, S. M., Cramphorn, C. J., Cameron, N. R., Gardner, P. M., Davis, B. G., Fernández-Trillo, F., and Alexander, C.: Synthetic polymers for simultaneous bacterial sequestration and quorum sense interference, Angew. Chem. Int. Ed., 50, 9852–9856, https://doi.org/10.1002/anie.201103130, 2011.

Zhang, D., Chen, Y., Zhao, Y., and Zhu, X.: New sludge pretreatment method to improve methane production in waste activated sludge digestion, Environ. Sci. Technol., 44, 4802–4808, https://doi.org/10.1021/es1000209, 2010.

Zhang, W., Liu, X., Liu, L., Lu, H., Wang, L., and Tang, J.: Effects of microplastics on greenhouse gas emissions and microbial communities in sediment of freshwater systems, J. Haz. Mat., 435, 129030, https://doi.org/10.1016/j.jhazmat.2022.129030, 2022.

Zhou, G., Shi, Q.-S., Huang, X.-M., and Xie, X.-B.: The three bacterial lines of defense against antimicrobial agents, Int. J. Mol. Sci., 16, 21711–21733, https://doi.org/10.3390/ijms160921711, 2015.